

Technical Report 1604

April 1993

Evaluation of the Production-Grade Class IV Flextensional Transducer Shell

J. D. Maltby

SUMMARY

OBJECTIVE

Evaluate physical characteristics and mechanical properties of the production-grade composite Class IV flextensional transducer shell produced by Brunswick Defense in Lincoln, NE.

RESULTS

The void content was very low; the average was $<0.5\%$. The fiber distribution was very uniform throughout the shell; the average fiber volume was 52%.

Interlaminar shear strength averaged 11.4 ksi. The shear modulus was very nonlinear. Its *initial* value was 0.52 Mpsi.

Through-the-thickness strength averaged 6.7 ksi in tension and 24.4 ksi in compression. Through-the-thickness test results revealed a nonlinear modulus in compression and a fairly linear modulus in tension.

CONCLUSIONS

The shell was of excellent quality and high strength. The through-the-thickness moduli were generally in good agreement with the analytically predicted values currently used in finite element modeling. However, the *initial* interlaminar shear modulus was more than 30% lower than the analytically predicted value. The disparity between the two increases as shear stress levels increase because of the nonlinear nature of the shear modulus. The effects of this disparity and the nonlinear moduli in general should be considered in current finite element models. Creep evaluation involving the mechanical test methods employed in this work would be useful in an analytical study to predict the useful life of the transducer shells (which will be dictated primarily by their creep performance, according to current operational practice).

CONTENTS

SUMMARY	i
SHELL DESCRIPTION	1
PHYSICAL CHARACTERIZATION TESTS	2
MECHANICAL PROPERTIES	4
INTERLAMINAR SHEAR TESTS	4
TEST DESCRIPTION	4
STRESS COMPUTATION	7
SHEAR SPECIMEN LOCATIONS	7
SHEAR TEST RESULTS	7
CYCLICALLY LOADED SPECIMEN	13
THROUGH-THE-THICKNESS MECHANICAL TESTS	15
LOCATIONS OF TEST SPECIMENS	17
TEST RESULTS	18
COMMENT ON THE TEST METHOD	19
CONCLUSIONS	19
REFERENCES	25

FIGURES

1. The regions of the test ring from which specimens were removed are depicted above	2
2. Iosipescu shear test fixture with gaged specimen. Notice the strain gage extends the full distance between the test specimen's notches	5
3. Geometry of tested Iosipescu specimens	6
4. Shear strain distribution across the test section depends on the orientation of the fibers. (The amount by which shear strain measured at the center of the test section deviates from the average shear strain across the full test section is greatly exaggerated in this figure.)	6
5. Locations of Iosipescu specimens	8

6.	<i>Raw load versus strain data for specimen Fi1I</i>	8
7.	<i>Load and strain versus time for specimen Fi1I</i>	9
8.	<i>Shear stress versus strain and tangent modulus versus stress for specimen CiI</i>	11
9.	<i>Shear stress versus strain and tangent modulus versus stress for specimen Fi1I</i>	11
10.	<i>Shear stress versus strain and tangent modulus versus stress for specimen Fi4II</i>	12
11.	<i>Shear stress versus strain and tangent modulus versus stress for specimen Fo4II</i>	12
12.	<i>Shear stress versus strain and tangent modulus versus stress for specimen Fi2I (on its first load cycle)</i>	13
13.	<i>Cyclic loading history for specimen Fi2I</i>	14
14.	<i>Raw load versus strain data for specimen Fi2I</i>	15
15.	<i>Geometry of tested through-the-thickness specimens</i>	16
16.	<i>A gripping fixture depicted above was bonded to each end of the through-the-thickness specimens</i>	16
17.	<i>Photo of through-the-thickness specimen situated in Instron test machine. Instron fixtures mate with gripping fixtures via pins slipped through holes</i>	17
18.	<i>Locations of through-the-thickness specimens</i>	18
19.	<i>Tensile stress versus strain and tangent modulus versus tensile stress for specimen F34</i>	20
20.	<i>Tensile stress versus strain and tangent modulus versus tensile stress for specimen F35</i>	21
21.	<i>Tensile stress versus strain and tangent modulus versus tensile stress for specimen T3</i>	21
22.	<i>Compressive stress versus strain and tangent modulus versus compressive stress for specimen C1. The specimen was cyclically loaded. Tangent moduli are plotted with respect to only the first cycle. The ultimate stress is not shown</i>	22
23.	<i>Stress versus strain for specimen F41. The specimen was cyclically loaded. The ultimate stress is not shown</i>	22
24.	<i>Tensile stress versus strain and tangent modulus versus tensile stress for first load cycle of specimen F41</i>	23

25.	<i>Compressive stress versus strain and tangent modulus versus compressive stress</i> for final load cycle of specimen F41. The ultimate stress is not shown	23
26.	One geometry of a rectangular through-the-thickness specimen	24

TABLES

1.	Results of physical characterization tests on Brunswick shell S/N 184	3
2.	Results of physical characterization tests on Brunswick shell S/N 11	3
3.	Shear strengths of tested specimens	10
4.	Tangent shear moduli at three arbitrary stress levels	13
5.	Tensile strengths and moduli of tested specimens	18
6.	Compressive strengths and moduli of tested specimens	19

APPENDICES

APPENDIX A	BRUNSWICK DEFENSE SPECIFICATIONS	A-1
APPENDIX B	TRANSDUCER SHELL INFORMATION	B-1

SHELL DESCRIPTION

The physical characteristics and mechanical properties of a typical production-grade composite shell segment used in a Class IV flextensional transducer were evaluated. Lockheed Sanders Surveillance Systems Division, Manchester, NH, prime contractor for the transducer, purchases these oval-shaped shells from Brunswick Defense, Lincoln, NE. Brunswick filament winds the shells out of fiberglass/epoxy. The particular shell segment under evaluation was manufactured by Brunswick in March of 1992 at which time they were under contract to build a production lot of transducer shells for Sanders. The purchased shell was specified to be built in the same manner and configuration as the production shells.

Brunswick assigned part number P/N 5705159P1, serial number S/N 184 to this shell segment. The shell's conformance data are found in appendix A. The purchased shell was the standard shell segment width of 8.67 inches.

The glass reinforcement used in the composite transducer shells is E-glass. The unidirectional fiber orientation is aligned perpendicular to the winding axis (i.e., "hoop" wound). Brunswick winds the shells on an aluminum mandrel.

We do not know the complete manufacturing details of the shells because Brunswick's process is proprietary. It is our understanding that the shells are filament wound with a preimpregnated E-glass tow that is made at Brunswick's facilities. Although Brunswick is known to use their own proprietary "wet" prepreg (i.e., nonstaged) in filament winding applications (reference 1), the prepreg used in these shells was, according to reference 2 (appendix B), staged to achieve better resin flow control. No doubt this aided in reducing the thickness disparity between the oval shell's end radii and midbay flats that normally results from the higher compaction occurring at the end curves during the winding process. Staging the prepreg should also have reduced the amount of resin bled off during cure and aided in achieving a more uniform fiber distribution.

Test specimens were removed from a 2.6-inch-wide ring section taken from the end of the shell segment. Prior to removing the test specimens, this ring was used to evaluate the shell's residual strains (reference 3). The regions from which the various test specimens were taken from the ring are depicted in figure 1.

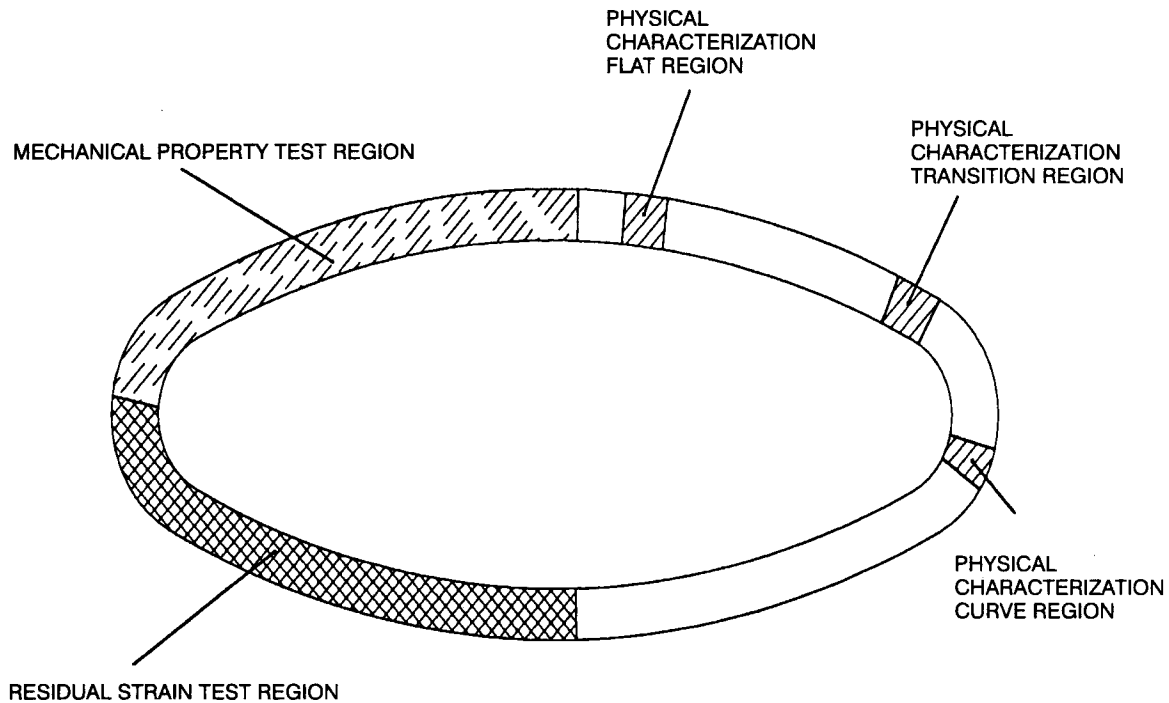


Figure 1. The regions of the test ring from which specimens were removed are depicted above.

PHYSICAL CHARACTERIZATION TESTS

Physical characterization consisted of measuring the material's specific gravity, fiber volume, and void content through the shell thickness (being near the *outside* shell surface, or in the *middle* of the shell thickness, or near the *inside* shell surface) at the *curve*, *flat*, and *transition* regions of the shell. Results of these tests are tabulated in table 1. References 4 and 5 were followed in determining these values.

This shell was observed to have a very low void content and an extremely uniform fiber distribution throughout.

A similar evaluation of the physical characteristics was conducted on another Brunswick shell that was made during the development phase of winding. The serial number of this second shell segment taken from the last developmental wind prior to the production run was S/N 11. The results for this shell are presented in table 2.

The results from this second shell are provided to reveal the good consistency in the material's physical characteristics that Brunswick achieved between the different times of shell manufacture, notwithstanding any minor process modifications that might have occurred between development and production.

Table 1. Results of physical characterization tests* on Brunswick shell S/N 184.

	# OF SPECS.	AVG. SPE. GRAV.	STND. DEV.	AVG. FIBER VOL. %	STND. DEV.	VARI-ANCE	AVG. VOID VOL. %	STND. DEV.	VARI-ANCE
Curve Outside	3	1.93	0.00	52.06	0.27	0.07	0.57	0.01	0.00
Curve Middle	3	1.93	0.01	52.11	0.39	0.16	0.60	0.01	0.00
Curve Inside	3	1.92	0.00	51.17	0.30	0.09	0.57	0.04	0.00
Trans. Outside	3	1.93	0.00	51.74	0.16	0.03	0.71	0.07	0.00
Trans. Middle	3	1.93	0.00	51.94	0.47	0.22	0.87	0.35	0.12
Trans. Inside	3	1.92	0.00	51.57	0.10	0.01	0.78	0.01	0.00
Flat Outside	3	1.93	0.00	51.72	0.12	0.01	0.62	0.03	0.00
Flat Middle	3	1.93	0.00	51.75	0.26	0.07	0.67	0.03	0.00
Flat In-side	3	1.93	0.00	51.80	0.03	0.00	0.68	0.04	0.00

Table 2. Results of physical characterization tests* on Brunswick shell S/N 11.

	# OF SPECS.	AVG. SPE. GRAV.	STND. DEV.	AVG. FIBER VOL. %	STND. DEV.	VARI-ANCE	AVG. VOID VOL. %	STND. DEV.	VARI-ANCE
Curve Outside	3	1.94	0.01	52.53	0.41	0.17	0.43	0.17	0.03
Curve Middle	3	1.94	0.00	52.45	0.22	0.05	0.47	0.02	0.00
Curve Inside	3	1.96	0.01	54.02	0.56	0.32	0.48	0.03	0.00
Trans. Outside	3	1.93	0.01	51.96	0.39	0.15	0.58	0.04	0.00
Trans. Middle	3	1.93	0.00	51.82	0.16	0.02	0.61	0.08	0.01
Trans. Inside	3	1.93	0.01	51.57	0.48	0.23	0.58	0.04	0.00
Flat Outside	3	1.93	0.01	51.66	0.13	0.02	0.73	0.32	0.10
Flat Middle	2	1.93	0.00	51.69	0.03	0.00	0.56	0.01	0.00
Flat In-side	3	1.93	0.00	51.68	0.27	0.07	0.59	0.03	0.00

*Values used in computations: fiber density — 2.620 g/cm³
resin density — 1.201 g/cm³

MECHANICAL PROPERTIES

Mechanical property tests consisted of measuring the interlaminar shear strength and moduli, and the through-the-thickness tensile and compressive strength and moduli. These properties are quite matrix dominated. Consequently, they are more reflective of the composite's processing quality, as opposed to the fiber-dominated, in-plane properties measured in the fiber direction (i.e., "unidirectional" properties).

"Unidirectional" properties were not measured; one reason is that they are difficult to acquire when the fibers are laid up on a curved surface. However, "unidirectional" modulus is reasonably predicted from the rule-of-mixtures. In-plane flexural strengths for the shells are measured by Brunswick (appendix A) and are believed to be adequate for current performance requirements.

The matrix-dominated properties tend to be nonlinear and even rate dependent and, therefore, not as easy to predict; yet their performance is considered crucial to the shell's structural integrity. Fortunately, fiber curvature is less of a problem in their evaluation if care is taken to align the fibers tangent to the specimen's gage section as described below.

INTERLAMINAR SHEAR TESTS

TEST DESCRIPTION

The Iosipescu shear test was used to evaluate interlaminar shear properties. The Iosipescu shear test requires the special test fixture pictured in figure 2. The geometry of the specimen and the dimensions specified for the tests are depicted in figure 3.

The Iosipescu shear test, also referred to as the "v-notch beam shear test," is becoming an accepted standard in the measurement of shear properties in anisotropic composite materials (reference 6). The test comes close to providing a state of pure shear between the notches. Not only does it provide shear strength, but shear modulus can also be obtained with the aid of strain gages mounted at the gage section between the notches. In contrast, the short-beam shear test does not induce a state of pure shear, nor does it provide an adequate means of determining the shear modulus. The American Society for Testing and Materials is planning to release the Iosipescu shear test method as standard D5379 in the near future.

Shear strain was measured with a new strain-gage rosette designed specifically for this test. The rosette consists of two strain gages, oriented at + and -45° to the shear plane. This new rosette differs from those previously available in that the filament grids span the entire distance between the notches of the specimen (figure 2). As a result, the rosette records the average or integrated shear strain across the entire test section. This tends to alleviate measurement problems that might be associated with any slight nonuniform shear stress profile existing between the notches. The nonuniform strain profile, which is dependent on the orientation of the fibers in the specimen, is illustrated (with exaggeration) in figure 4. This new gage also has low sensitivity to misalignment and is able to sample a sufficiently large area to account for any local variations in material properties.

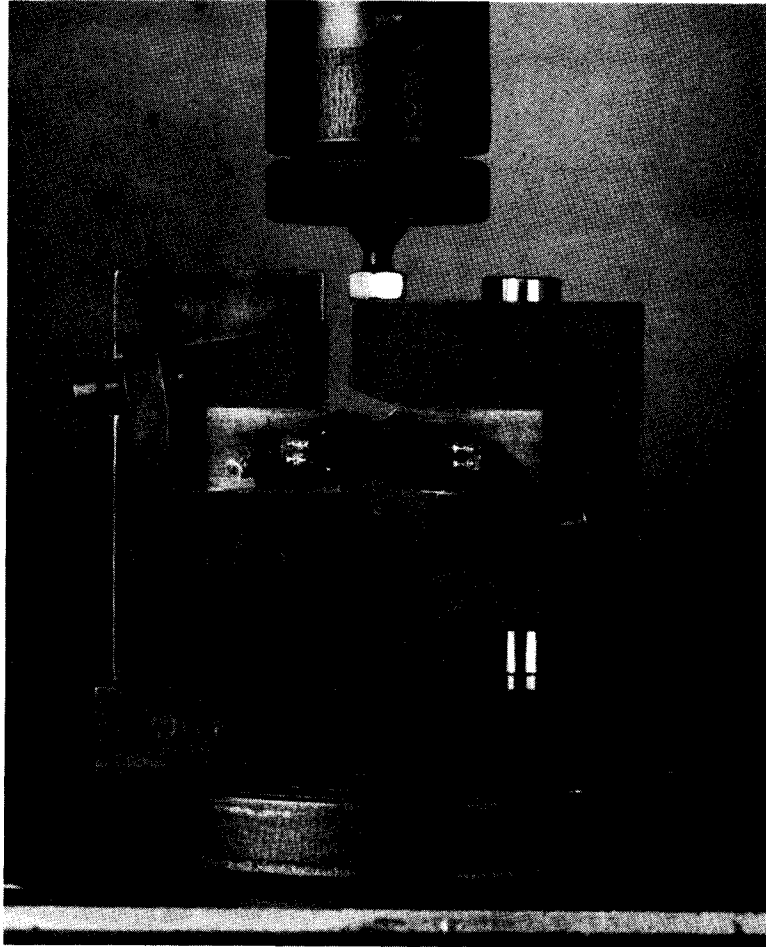


Figure 2. Iosipescu shear test fixture with gaged specimen. Notice the strain gage extends the full distance between the test specimen's notches.

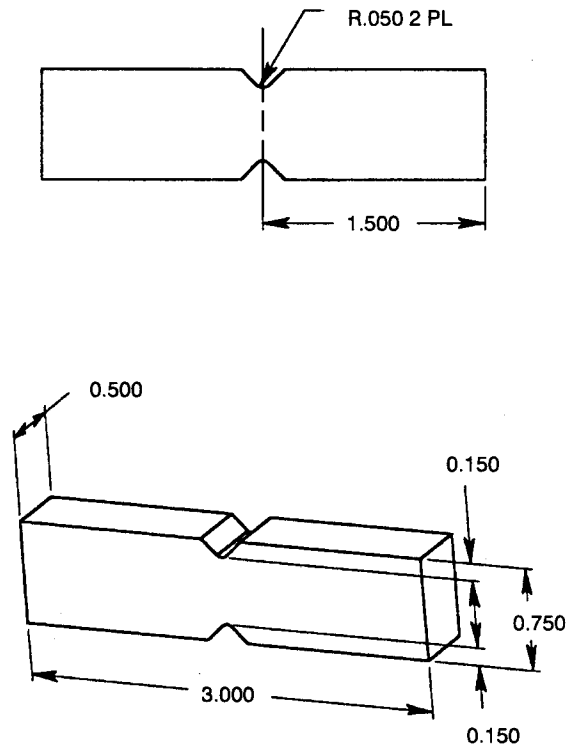


Figure 3. Geometry of tested Iosipescu specimens.

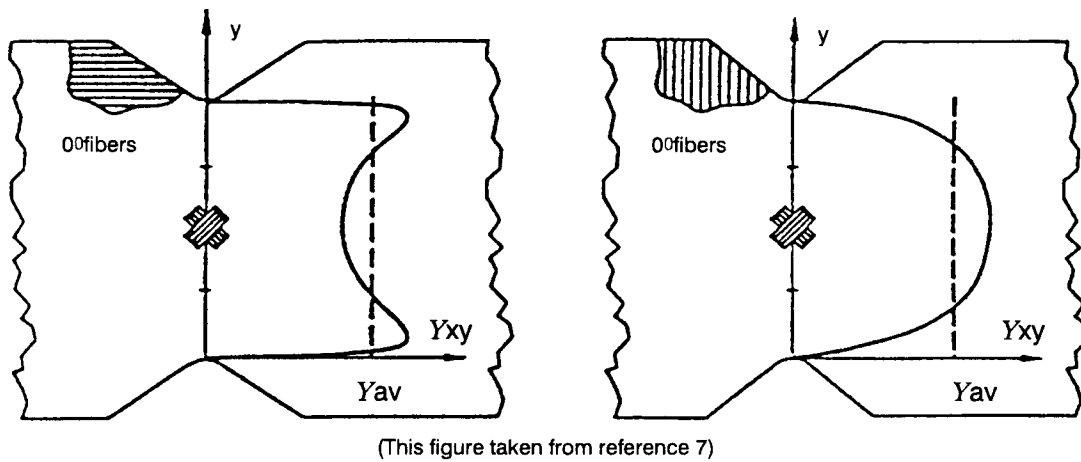


Figure 4. Shear strain distribution across the test section depends on the orientation of the fibers. (The amount by which shear strain measured at the center of the test section deviates from the average shear strain across the full test section is greatly exaggerated in this figure.)

STRESS COMPUTATION

In the Iosipescu shear test, shear stress is calculated by dividing the applied load, P , by the specimen's cross-sectional area between the notches

$$\begin{aligned} \tau_{12} &= P/(wt), \\ \text{where} \quad w &= \text{distance between the notches,} \\ \text{and} \quad t &= \text{specimen thickness.} \end{aligned} \tag{1}$$

Shear strain, γ_{12} , is determined from the strains measured on the 45° gages according to

$$\gamma_{12} = |\epsilon_{45} - \epsilon_{45}|, \tag{2}$$

which, in a state of pure shear, is essentially twice the magnitude of strain recorded on one gage. (Nevertheless, Lee and Munro [reference 8] recommend that both the tensile and compressive gages should be monitored separately to insure that a state of pure shear exists under the gage.)

Shear modulus, G_{12} , is simply

$$G_{12} = \tau_{12}/\gamma_{12}. \tag{3}$$

As we will see in the results, the slope of the shear stress versus strain curve for this material is nonlinear. Therefore, the shear modulus needs to be expressed as a *tangent modulus* at a given stress level (which is the slope of the stress versus strain curve at that stress level).

SHEAR SPECIMEN LOCATIONS

Locations of the tested specimens are shown in figure 5. Care was taken to align the fibers such that they were tangent to the midplane of the test specimen at the shear plane, as illustrated on specimens CiI and Fi4II in figure 5. Specimens were visually inspected after machining to check for proper fiber alignment.

SHEAR TEST RESULTS

Figure 6, a plot of the raw strain-gage test data for specimen Fi1I, illustrates some typical behavior observed in the tests. Notice the symmetrical strain behavior recorded on the two gages (i.e., where strains measured by each gage are very similar—except of course for their sign), which is evidence that a strain state close to pure shear exists under the gage.

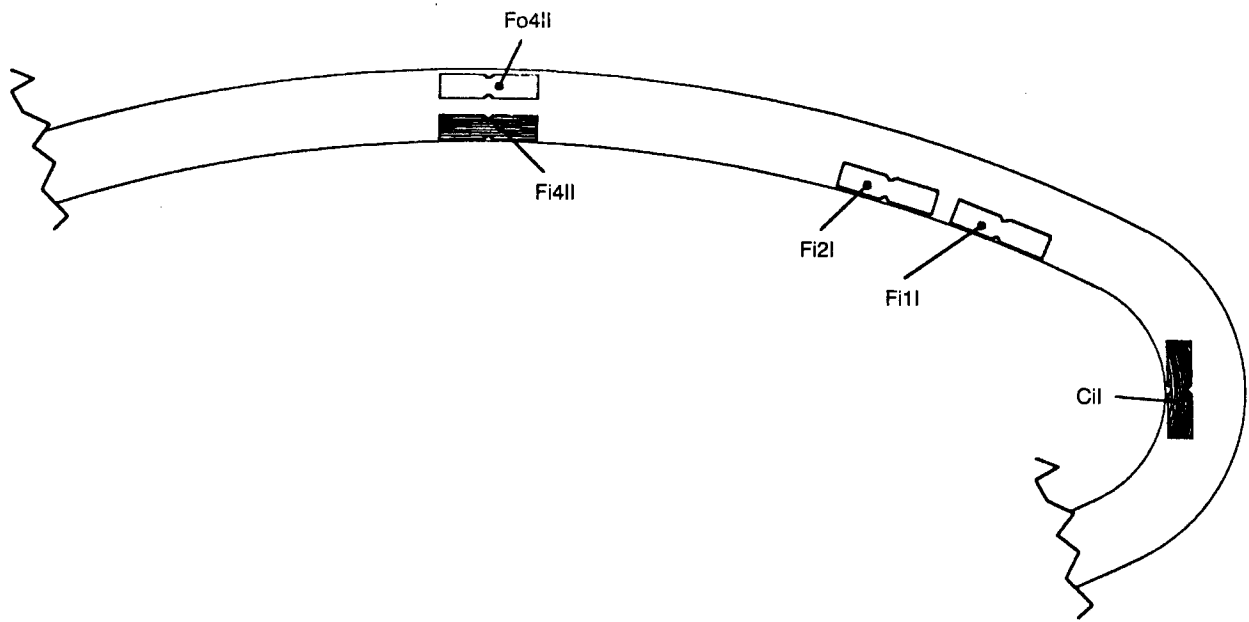


Figure 5. Locations of Iosipescu specimens.

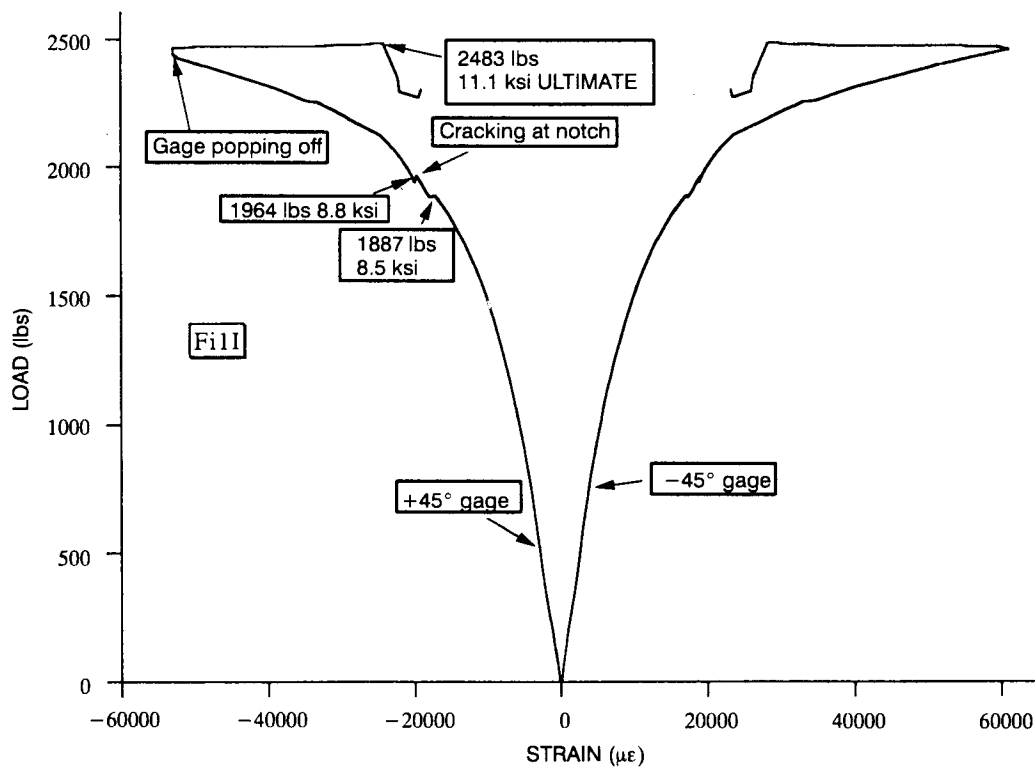


Figure 6. Raw load versus strain data for specimen Fi1I.

The gage adhesive was typically only good for about 6% *measured* strain (i.e., 12% *shear* strain), at which point the gages popped off of the specimens. Therefore, ultimate strain values were not recorded. However, load versus time plots (e.g., figure 7) are useful to ascertain the complete loading response through ultimate load. Raw strain recorded for the -45° gage is also plotted as a function of time in figure 7. By extrapolating the strain curve beyond the point at which the gage was lost, a reasonable estimate of the ultimate strain can be obtained, which, for this specimen, was approximately 7.5% *measured* (i.e., 15% *shear* strain). Following this same procedure, the ultimate shear strain was found to be close to 18% shear strain on specimens Fi4II and Fo4II.

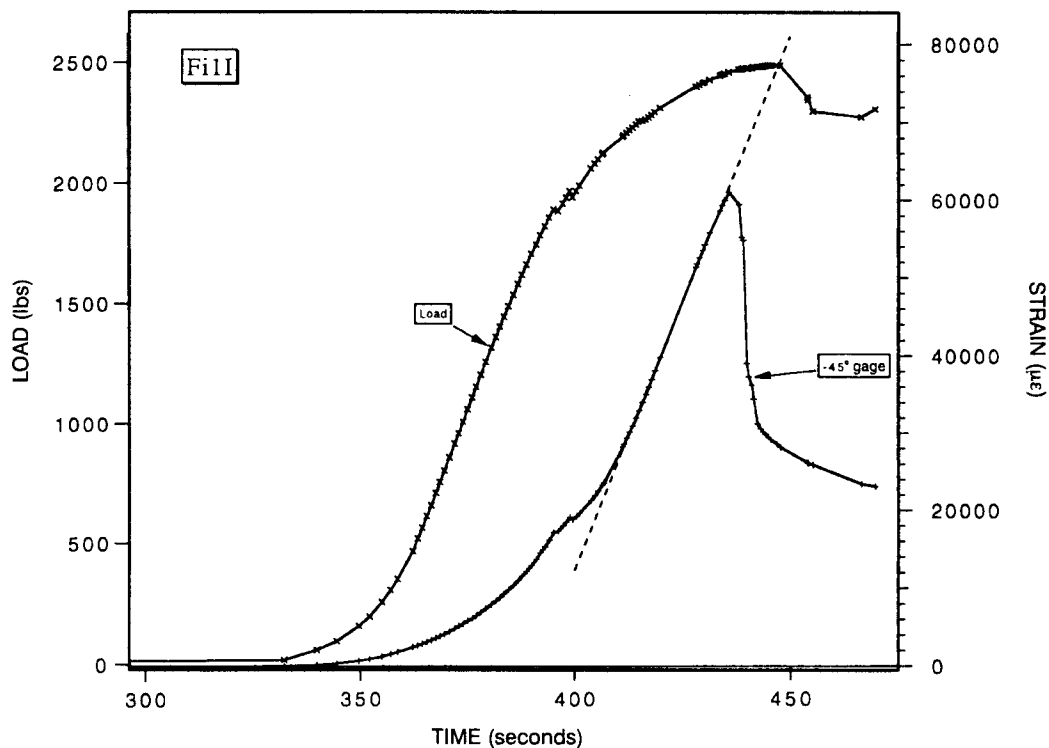


Figure 7. *Load and strain versus time* for specimen Fi1I.

Another characteristic common to all of these tests is the momentary load drop(s) that occurs in the range of 70-80% of the ultimate test load. These load drops (that occurred at 1887 pounds and 1964 pounds for this particular specimen) are attributable to cracks initiating at the notch roots. The drops can be quite audible.

The stress at which cracks develop at the notch root loci should not be construed as the specimen's strength. As depicted in figure 4, testing a composite Iosipescu specimen such that the fiber direction is oriented perpendicular to the loading direction results in a stress concentration occurring at the notches. It was found through the work of reference 9, which included both empirical testing and analytical finite element modeling, that the "...cracks at the notch root tended to relieve the shear stress concentration, as would be expected. However, these cracks did not significantly alter the stress state in the test region..."

For our tests, it is reasonable to base the shear strength on the ultimate load obtained by the specimen. Shear strength values based on ultimate load for all specimens tested are expressed in table 3.

Table 3. Shear strengths of tested specimens.

Specimens:	Shear Strength (ksi)
CiI	11.9
Fi1I	11.1
Fi4II	11.5
Fo4II	10.8
Fi2I	11.7
AVERAGE:	11.4

Shear stress and strain were reduced from the raw data according to equations (1) and (2). The shear stress versus shear strain curves for all of the specimens are shown in figures 8 through 12.

As previously noted, the stress versus strain curves do not display a region of linearity, so the shear modulus needs to be expressed in terms of a particular stress or strain level. Tangent modulus values are also plotted versus stress in figures 8 through 12. Tangent modulus is the slope of the stress versus strain curve, $\Delta\tau/\Delta\gamma$, between points i and successively acquired j . Thus, the tangent modulus at point j (e.g., G_{12j}) was determined as follows:

$$G_{12j} = (\tau_{12j} - \tau_{12i})/(\gamma_{12j} - \gamma_{12i}).$$

It is observed on all of the tangent modulus plots that when the specimen is initially loaded, there is a period of adjustment, up to about a stress level of 2000 psi, for which it is difficult to ascertain consistent tangent modulus values because of their relatively large variation. Beyond that level, the tangent moduli tend to monotonically decrease with increasing stress level (neglecting any relatively minor point-to-point fluctuation).

Tangent modulus is presented in table 4 for all the specimens at three arbitrary stress levels. All of the specimens were observed to be fairly consistent, and no significant change existed between cycles for specimen Fi2I even after being subjected to sustained periods of holding under load.

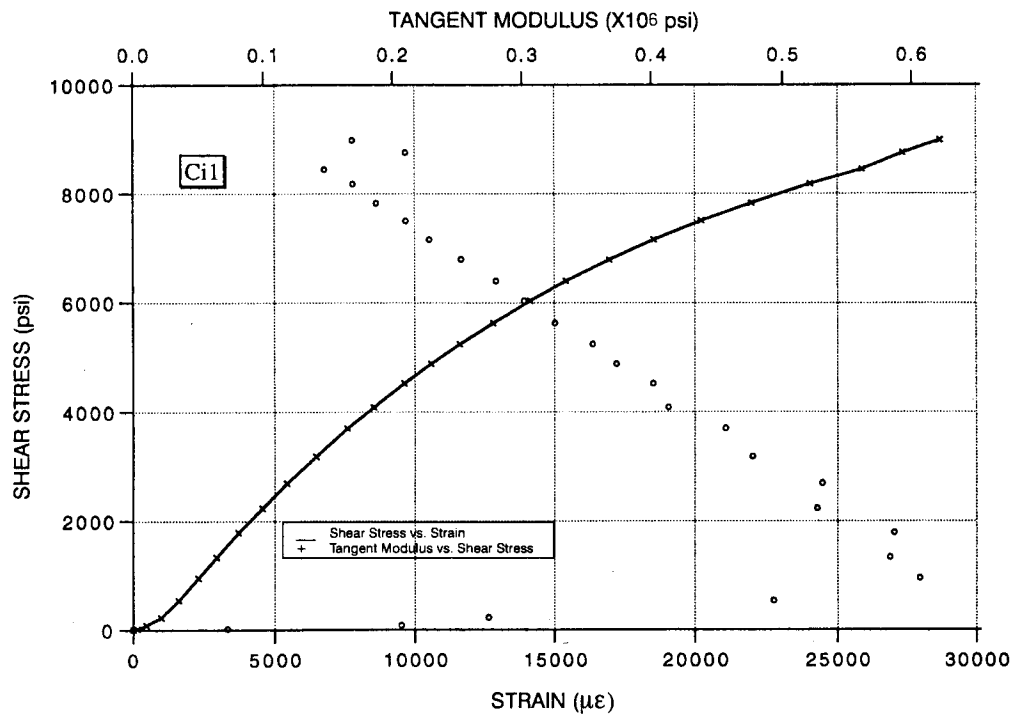


Figure 8. *Shear stress versus strain and tangent modulus versus stress for specimen CiI.*

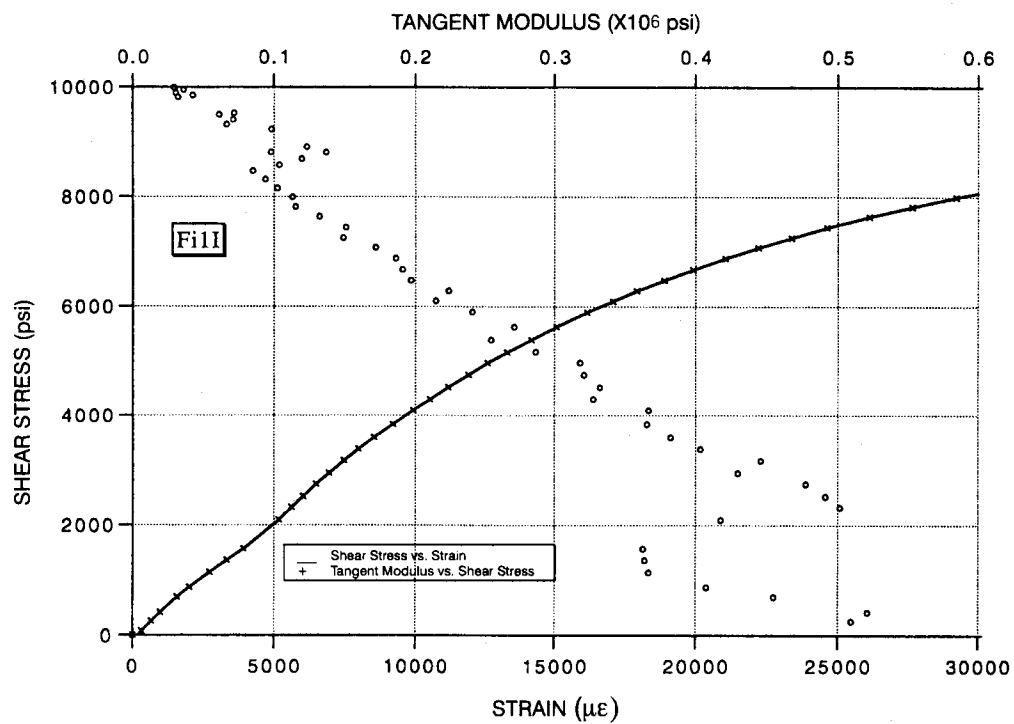


Figure 9. *Shear stress versus strain and tangent modulus versus stress for specimen FiII.*

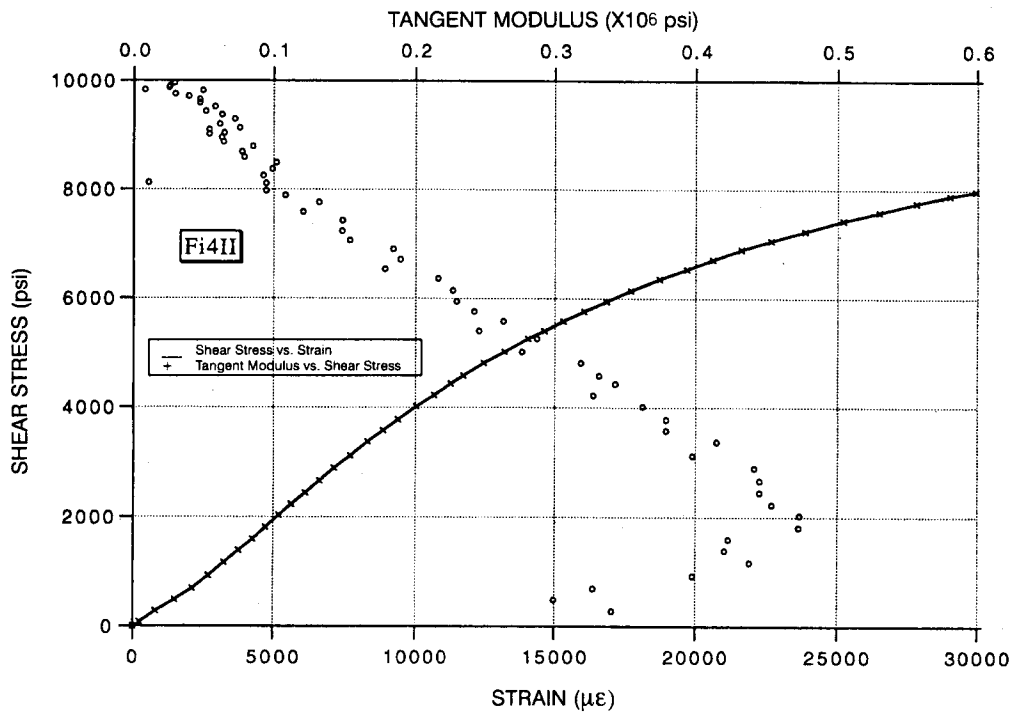


Figure 10. *Shear stress versus strain and tangent modulus versus stress for specimen Fi4II.*

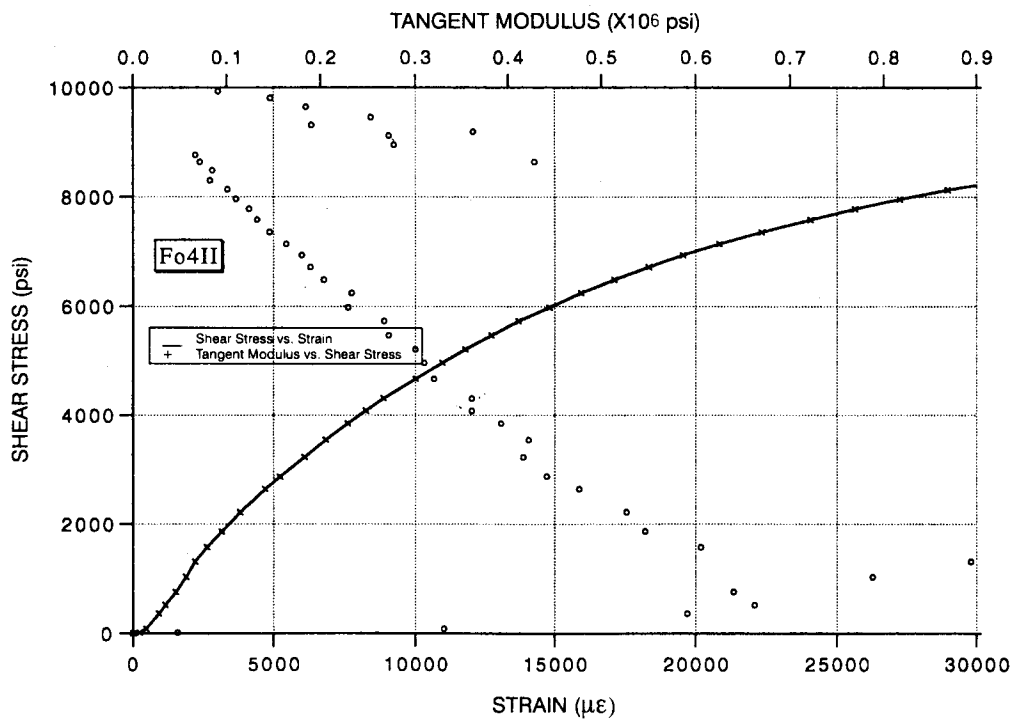


Figure 11. *Shear stress versus strain and tangent modulus versus stress for specimen Fo4II.*

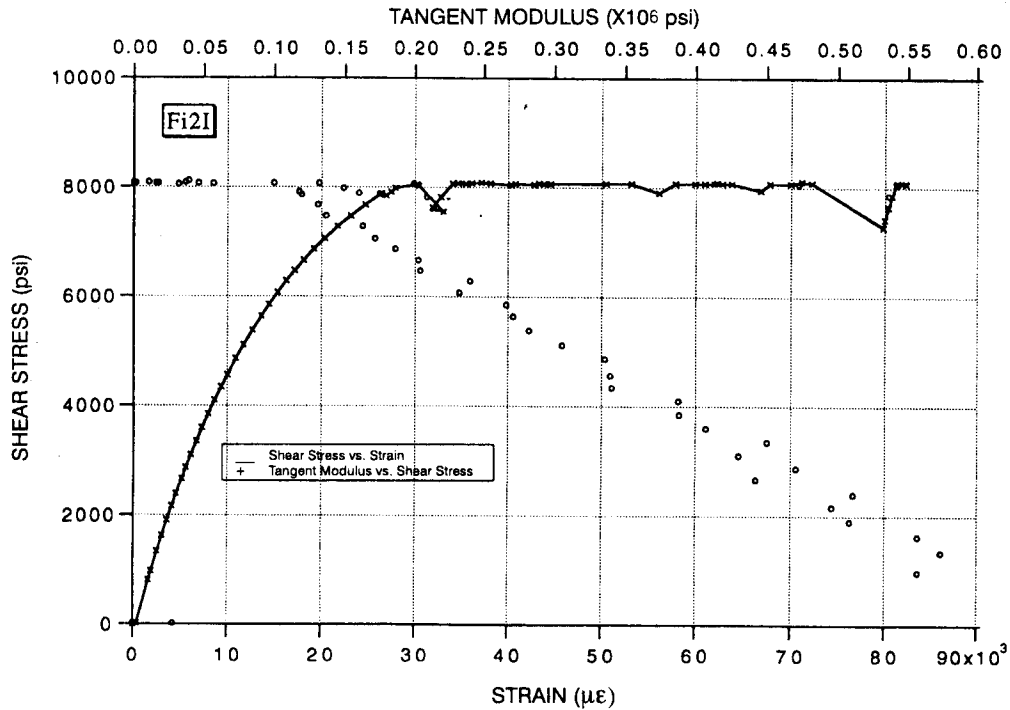


Figure 12. *Shear stress versus strain and tangent modulus versus stress for specimen Fi2I (on its first load cycle).*

Table 4. Tangent shear moduli at three arbitrary stress levels.

Respective Specimen's TANGENT SHEAR MODULI (Mpsi):									
STRESS LEVEL	CiI	Fi1I	Fo4II	Fi4II	Fi2I				Average of 5* specs.
					Cycle 1	Cycle 2	Cycle 3	Cycle 4	
2,000 psi	0.55	0.52	0.55	0.47	0.52	0.47	0.48	0.54	0.52
5,000 psi	0.37	0.30	0.30	0.30	0.31	0.27	0.28	0.32	0.32
8,000 psi	0.18	0.11	0.11	0.11	0.12	0.14	0.15	0.14	0.13

*Specimen Fi2I's cycle 1 values used in average.

CYCLICALLY LOADED SPECIMEN

Specimen Fi2I was reserved for special evaluation. The specimen was cyclically loaded to observe its creep characteristics when held at a stress value substantially below the typical shear strength of the other specimens.

The cyclical load history for specimen Fi2I is found in figure 13. On cycle 1, the specimen was taken to approximately 1850 pounds (8000 psi shear stress) and held for about one day. On cycle 2, the specimen was held at that same level for over 15 hours. It was held again at the same load level for an additional 5 hours in cycle 3. In cycle 4, the specimen was taken to failure.

During the hold period, significant load relaxation occurred because of creep in the specimen. Eventually, the load was manually readjusted to the initial hold load. But large load drops are observed in cycles 1 and 2 when the specimen was left unattended overnight.

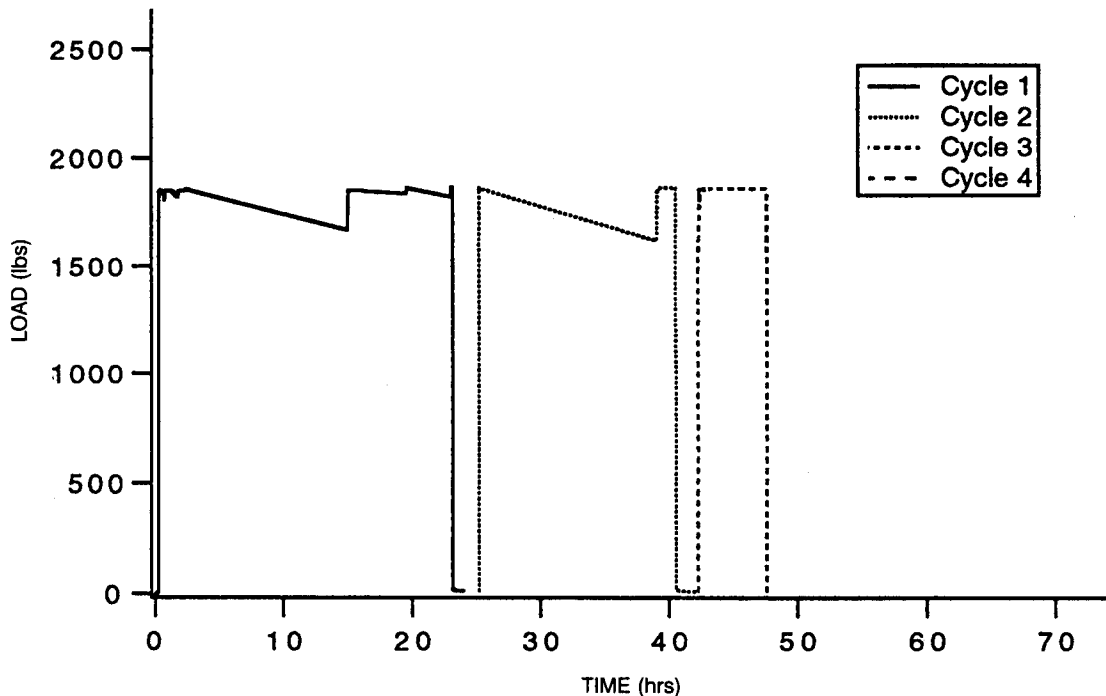


Figure 13. Cyclic loading history for specimen Fi2I.

The strain response for these four cycles is plotted in figure 14. Creep during the hold periods is seen, as well as some elastic recovery, when the load was removed. The total creep strain that occurred over the three hold periods—about 9% *shear* strain (i.e., 4,500 $\mu\epsilon$ *measured*)—was substantial for a total hold period of relatively short duration (being less than 50 hours total). However, the specimen was still able to sustain an ultimate stress of 11.7 ksi on the final load cycle, comparable to strengths measured on the other specimens. The reason for the apparent lack of the creep's affect on strength might be attributable to the fact that the total creep strain was only 50% of the ultimate strain magnitudes observed on some of the other specimens. Lower ultimate strengths might be observed if test specimens were exposed to a longer hold period in which creep strain was allowed to approach the typical ultimate strain magnitude.

One conclusion we might draw from this (albeit cursory) review of the creep shear response is the indication that the shear modulus is, to some extent, a function of the strain rate. Obviously, if the material was loaded very slowly in order for creep to occur (e.g., over a period of a couple of days) up to a stress level of 8,000 psi, the resulting strain magnitudes would be much higher and thus the tangent moduli would be lower.

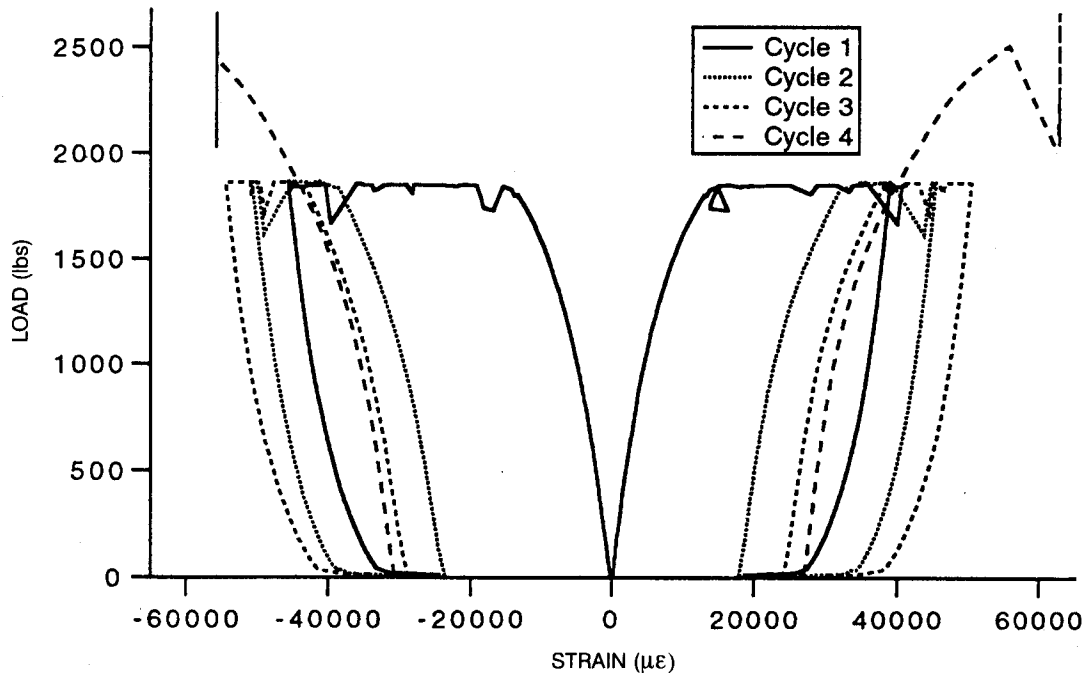


Figure 14. Raw *load versus strain* data for specimen Fi2I.

THROUGH-THE-THICKNESS MECHANICAL TESTS

A test method and specimen to determine the shell's mechanical properties in its thickness direction was developed. Since the shell was only two inches thick, a nonstandard test specimen was required. Gripping fixtures for the test specimen were also designed in conjunction with the specimen so that they both functioned collaterally for application in either compression or tension tests.

A "dumbbell-shaped" round geometry was selected for the specimen (figure 15) primarily because it was believed that good alignment could be more readily achieved with a turned specimen. The center gage region of the specimen was made long enough to place a strain gage rosette of size sufficient to facilitate handling.

Identical gripping fixtures (figure 16) were designed for each end of the specimen as the means of transferring the load from the test machine to the specimen. The specimens were adhesively bonded to the bottom of the countersunk hole in the fixture. Three equally spaced drill holes were made around the circumference of this hole so that adhesive would flow up and around the end of the specimen. The adhesive was fast setting and strong, a methyl-2-cyanoacrylate.

After testing, the specimen remnants were removed from the gripping fixtures by burning them out in a muffle furnace. The fixtures were lightly grit blasted and cleaned with alcohol prior to their reuse. The fixtures were made of an extra-low-carbon stainless steel to minimize any corrosive or oxidative action from repetitive burn-offs.

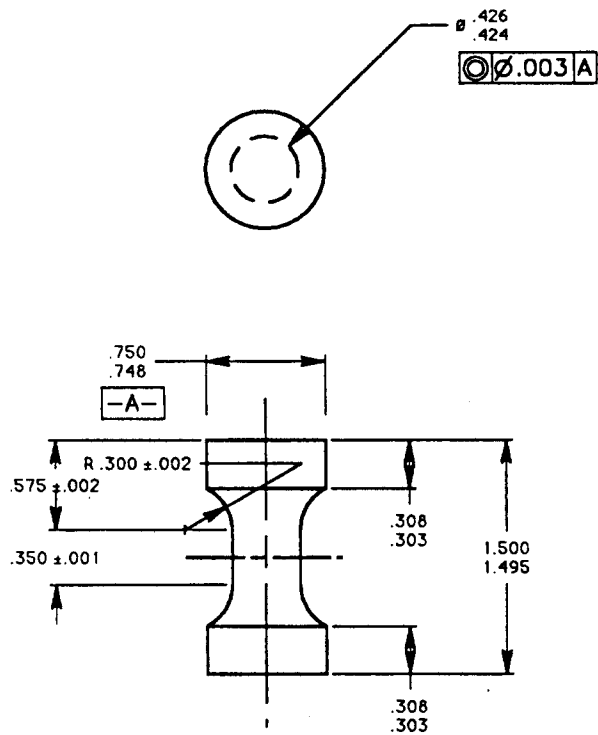


Figure 15. Geometry of tested through-the-thickness specimens.

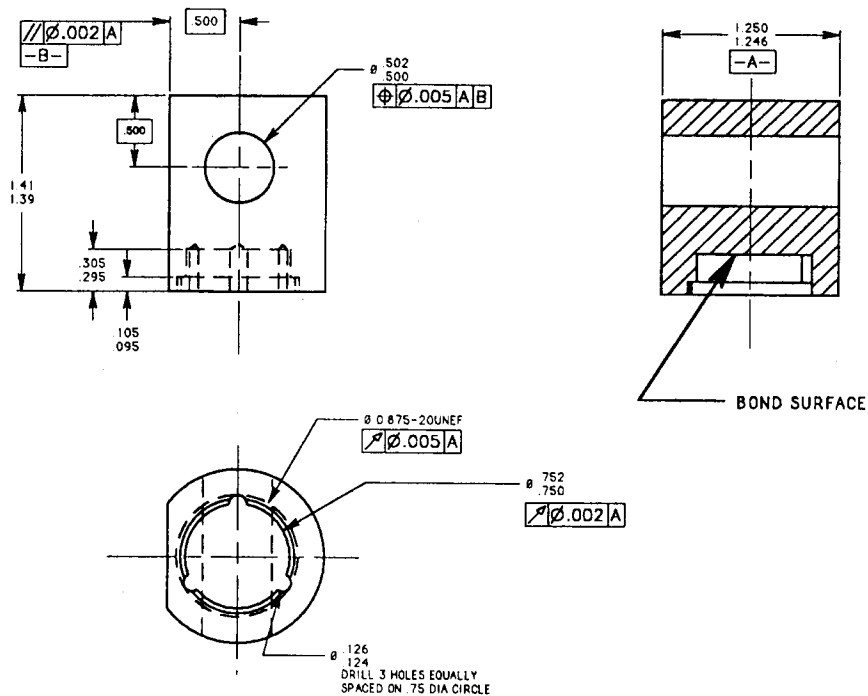


Figure 16. A gripping fixture depicted above was bonded to each end of the through-the-thickness specimens.

The gripping fixtures mated with standard INSTRON test fixtures in which they were held by pins slipped into the holes on the side of the fixtures (figure 17). The machined flats on the side of the fixtures were used to properly align the fixture holes during the bonding process.

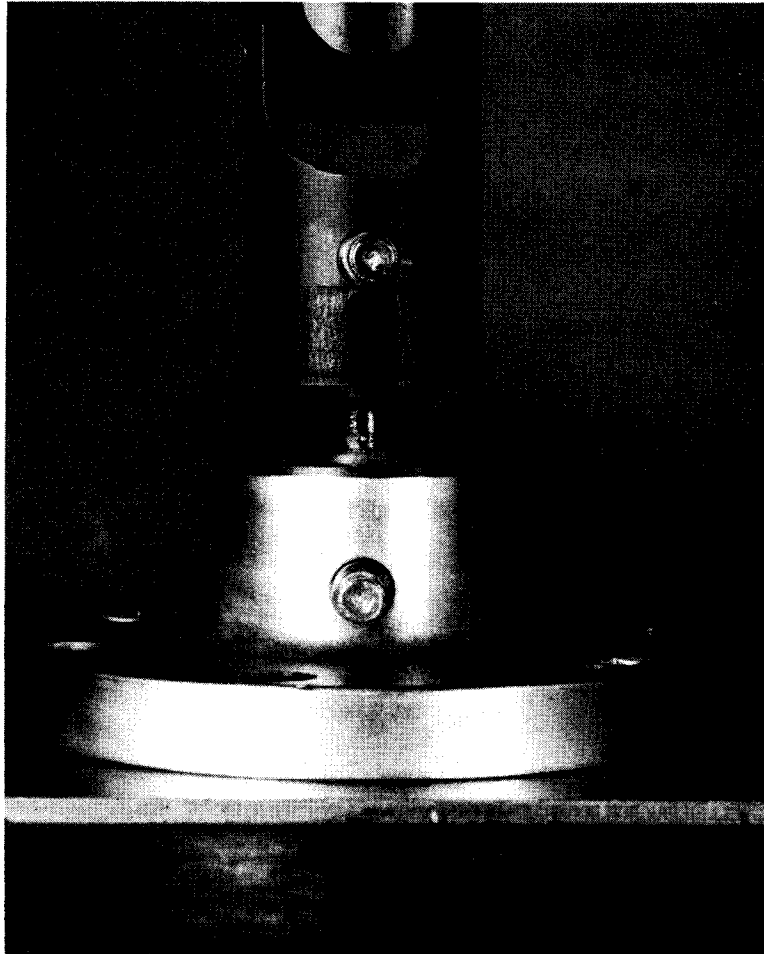


Figure 17. Photo of through-the-thickness specimen situated in Instron test machine. Instron fixtures mate with gripping fixtures via pins slipped through holes.

LOCATIONS OF TEST SPECIMENS

The respective locations of the tested specimens are shown in figure 18. Care was taken in machining to orient the specimens such that the composite's fibers were perpendicular to the specimen's longitudinal axis through the gage region.

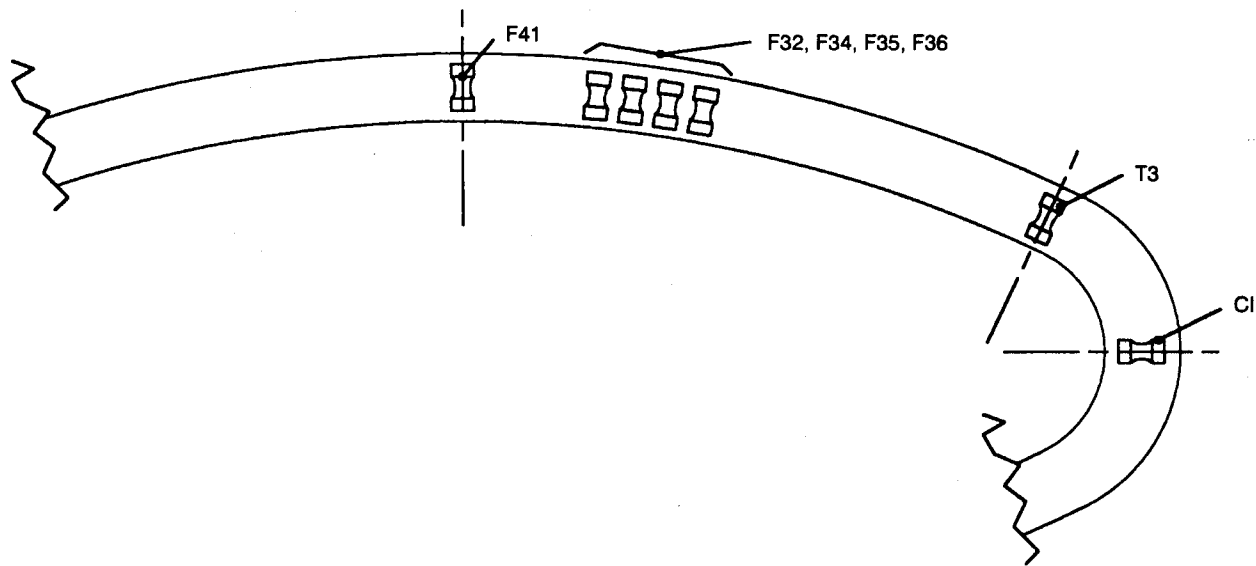


Figure 18. Locations of through-the-thickness specimens.

TEST RESULTS

Stress versus strain is plotted in figures 19 through 23 for five of the seven specimens tested. Also plotted are tangent moduli versus stress.

Results are tabulated in table 5 for the five specimens tested in tension. Excessive bending was concluded from the strain data for three of the specimens. A modulus measurement was not considered valid for two of those specimens as noted in table 5.

Table 5. Tensile strengths and moduli of tested specimens.

Specimens:	Tensile Strength (ksi)	Tensile Modulus [†] (Mpsi)
F32 [^]	7.4	[^]
F34 [^]	5.1	1.4
F35	7.6	1.4
F36 [^]	6.7	[^]
T3	6.8	1.6
C1	•	1.6
AVERAGE:	6.7*	1.5**

[†]Tangent modulus at 2500 psi.

[^]Severe bending occurred in specimen.

•Not taken to failure in tension.

*Average of five specimens.

**Average of four specimens.

Table 6 lists the results for the two specimens tested in compression. As seen in figures 22 and 23, both of the specimens tested in compression were cyclically loaded. The tangent moduli data plotted for C1 in figure 22 is with regard to only the first compression cycle.

Table 6. Compressive strengths and moduli of tested specimens.

Specimens:	Compressive Strength (ksi)	Compressive Modulus [†] (Mpsi)
F41*	24.1	1.7
C1*	24.6	1.6
AVERAGE:	24.4	1.7

[†]Tangent modulus at 2500 psi.

*Specimen was cycled.

The first cycle for specimen F41 (figure 23) was the tension cycle to a stress level of 6.7 ksi. Subsequently, the specimen was loaded in compression to successively higher stress levels until it failed at 24.1 ksi. Tangent moduli of specimen F41 are plotted in figure 24 for the first tension cycle and in figure 25 for the last compression cycle.

COMMENT ON THE TEST METHOD

One drawback of using a round specimen was the inability to obtain a meaningful measurement of Poisson's ratio because of the specimen's orthotropic nature. In retrospect, a rectangular "dog-bone-shaped" specimen (figure 26) may be a more useful test geometry for testing through-the-thickness properties. Poisson's ratio for both transverse directions could be measured with such a specimen.

CONCLUSIONS

The shell was of excellent quality with a low void content averaging <0.5% and uniform fiber distribution throughout.

The interlaminar shear strength measured with the Iosipescu method averaged 11.4 ksi, which is a little lower than the 12.96 ksi measured by Brunswick according to the short-beam shear method (appendix A). Nonetheless, shear strength, as well as through-the-thickness strength, were very good.

The through-the-thickness moduli were generally in good agreement with the analytically predicted values currently used in finite element modeling, notwithstanding the nonlinear nature of the modulus when measured in compression. However, the initial interlaminar shear modulus was more than 30% lower than the analytically predicted value. The disparity between the two increases as shear stress levels increase because of the nonlinear nature of the shear modulus. The effects of the nonlinear moduli on current shell stress and global performance predictions should be considered in the finite element models.

Admittedly, this review is brief, but it gives a glimpse of what can be expected in the mechanical properties that are of most interest to the shell's performance. It also confirms that

significant creep in shear can occur at substrength levels. Creep in through-the-thickness properties, although not looked at, is also potentially significant to the shell performance.

The effective useful life of the transducer will most likely be determined by the shell material's creep characteristics; creep in the shell will relieve the compressive prestress on the ceramic stack. Effective creep rates in the shells could be predicted in finite element models by stepwise application of localized creep using information garnered from creep test coupons similar to those employed in this work.

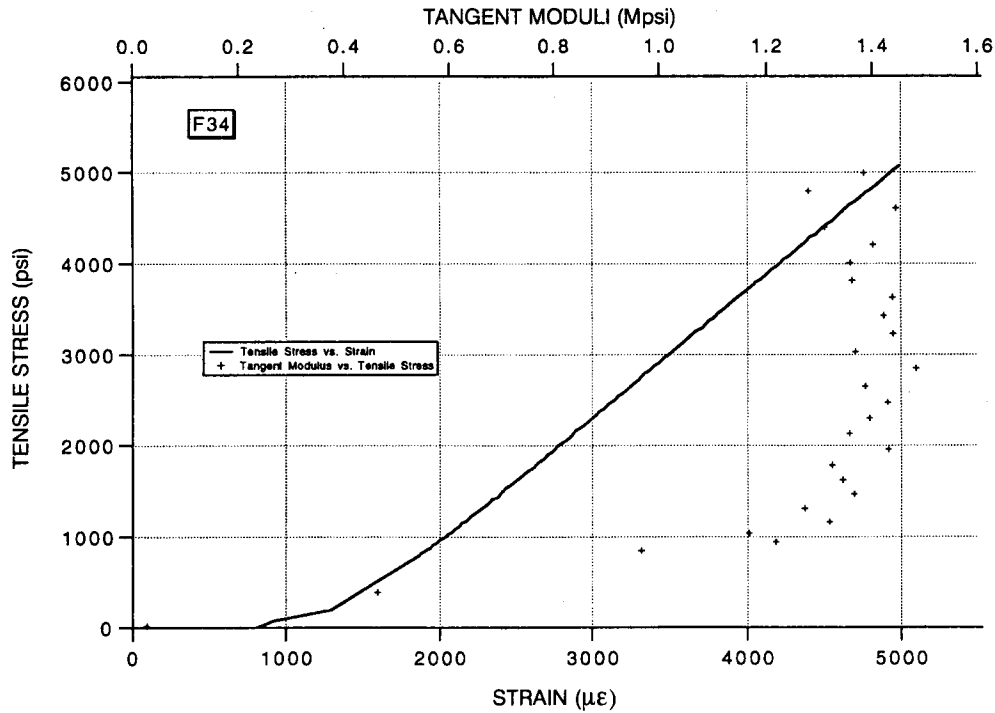


Figure 19. Tensile stress versus strain and tangent modulus versus tensile stress for specimen F34.

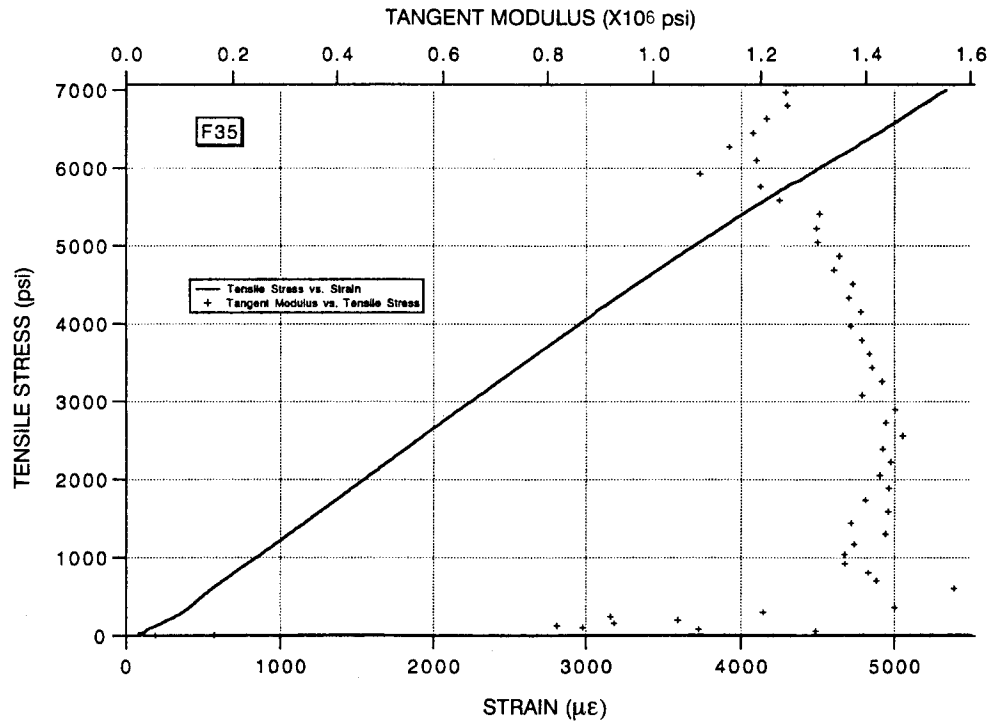


Figure 20. Tensile stress versus strain and tangent modulus versus tensile stress for specimen F35.

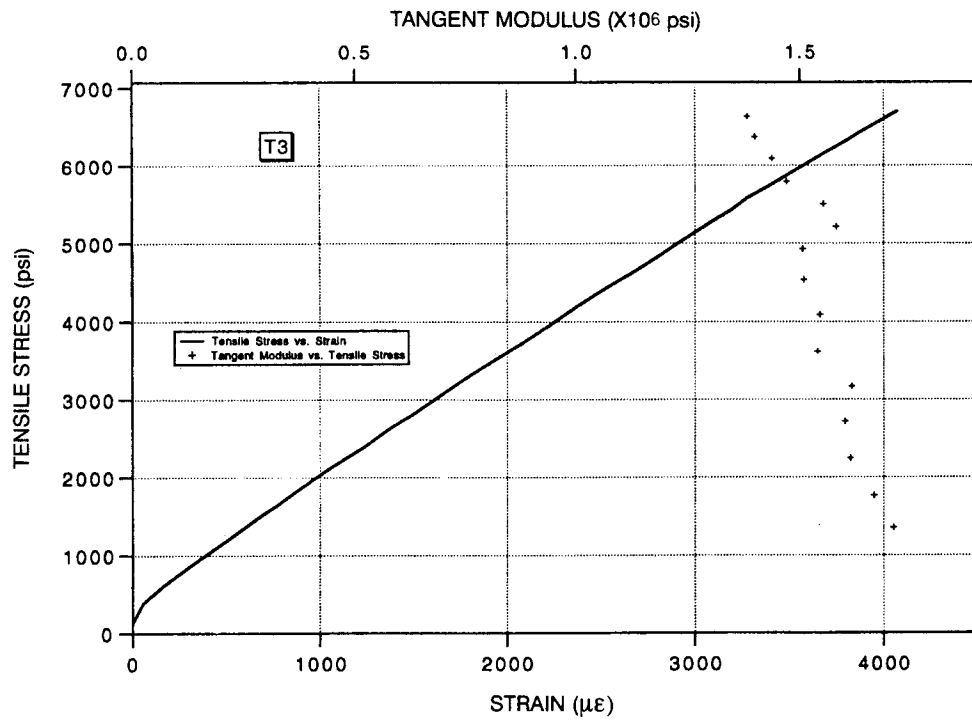


Figure 21. Tensile stress versus strain and tangent modulus versus tensile stress for specimen T3.

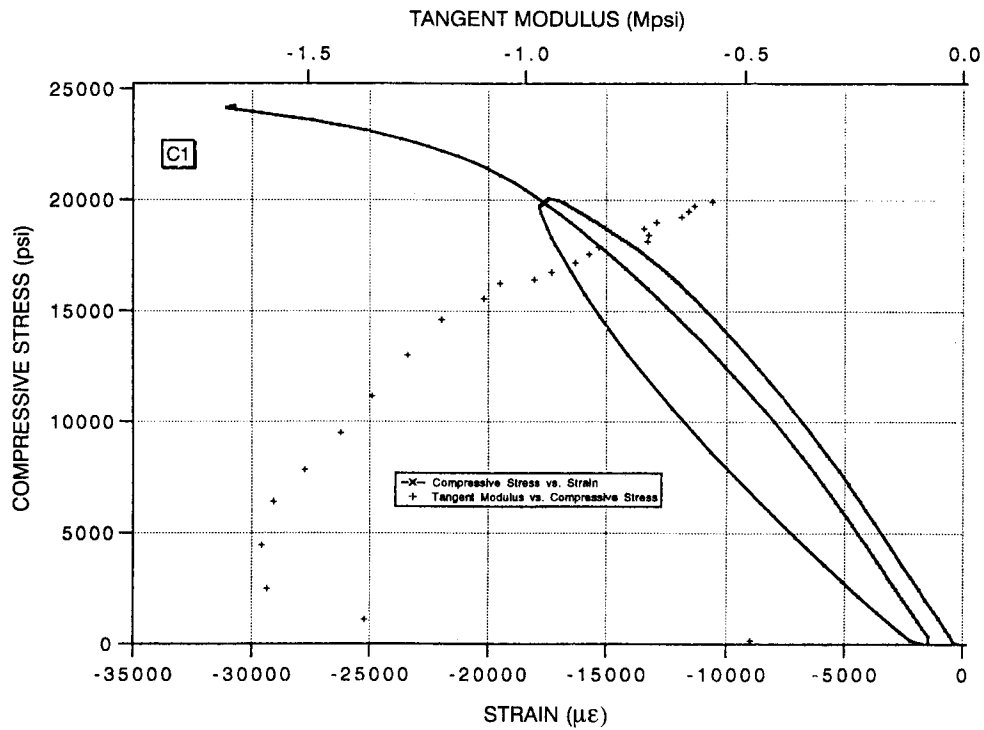


Figure 22. *Compressive stress versus strain and tangent modulus versus compressive stress* for specimen C1. The specimen was cyclically loaded. Tangent moduli are plotted with respect to only the first cycle. The ultimate stress is not shown.

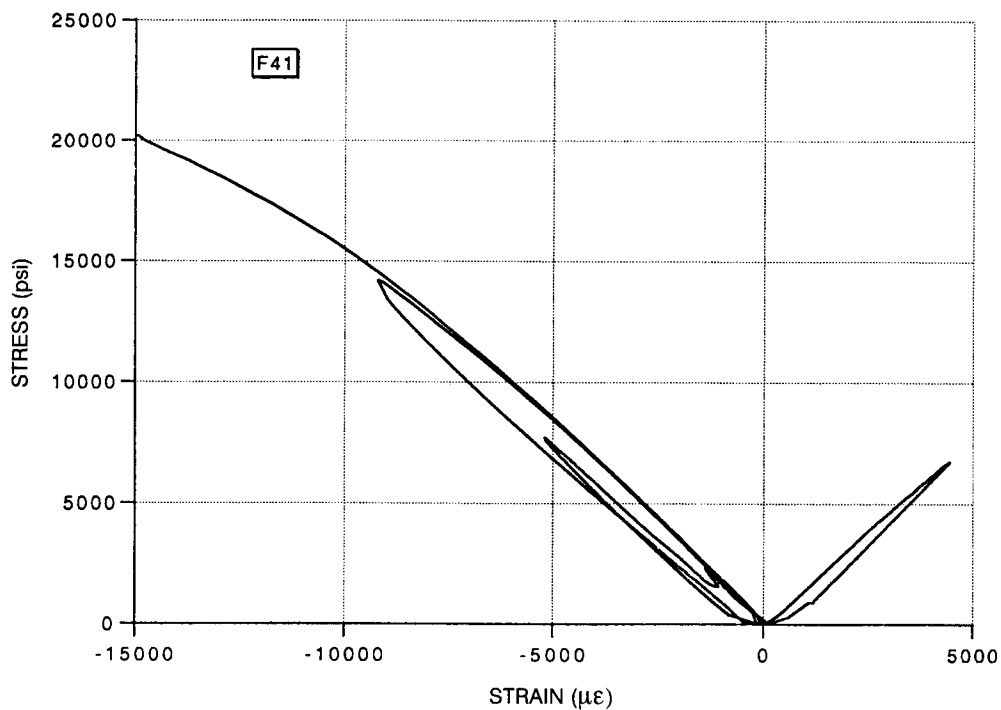


Figure 23. *Stress versus strain* for specimen F41. The specimen was cyclically loaded. The ultimate stress is not shown.

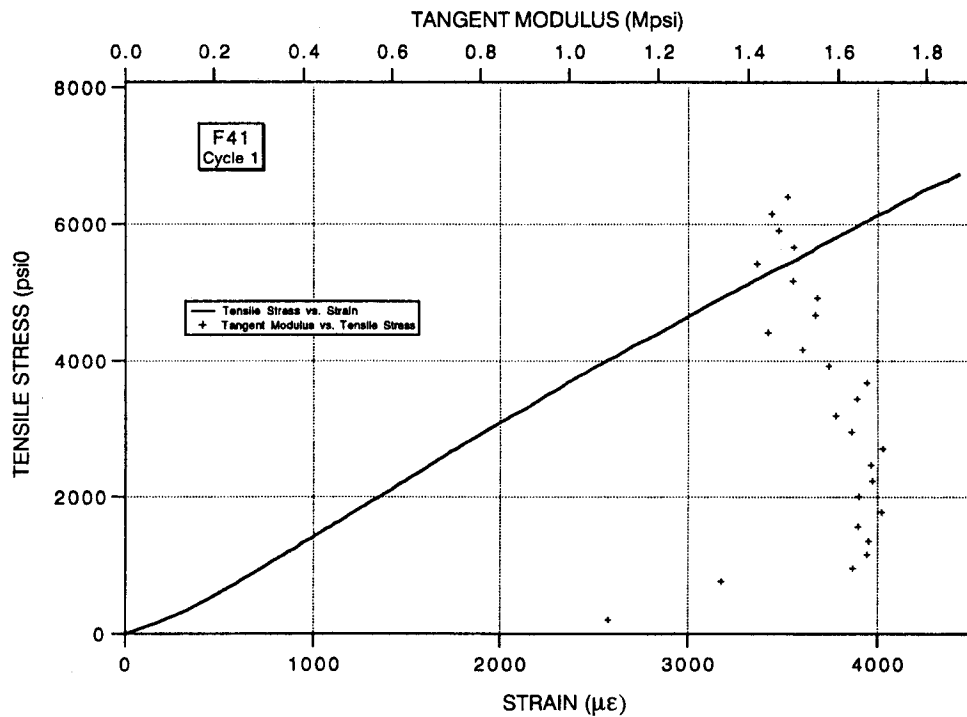


Figure 24. *Tensile stress versus strain and tangent modulus versus tensile stress* for first load cycle of specimen F41.

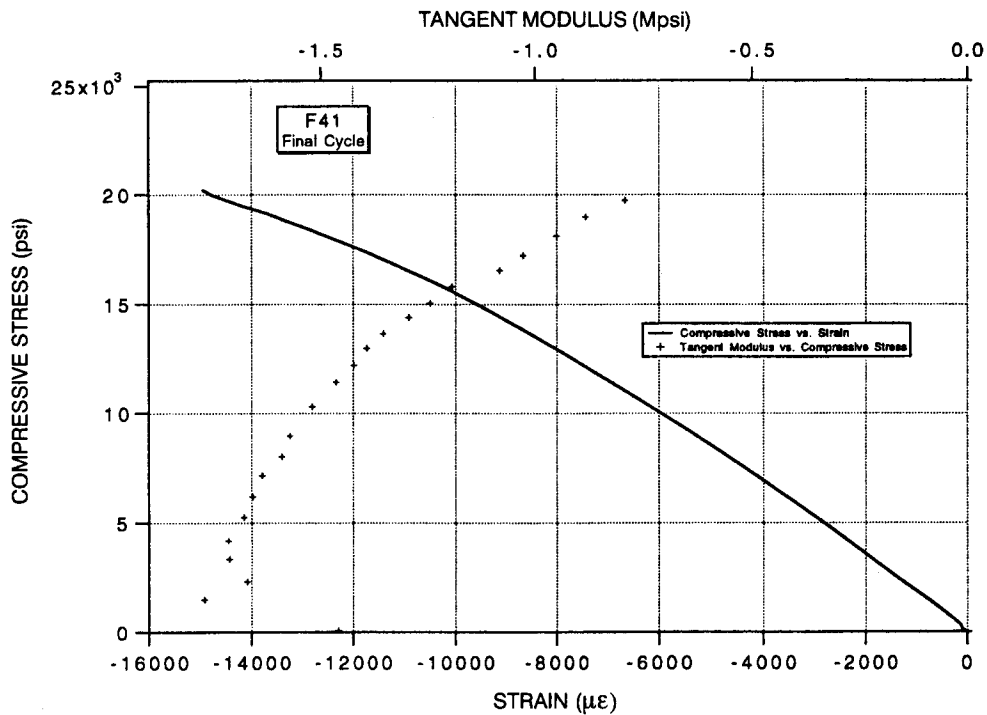


Figure 25. *Compressive stress versus strain and tangent modulus versus compressive stress* for final load cycle of specimen F41. The ultimate stress is not shown.

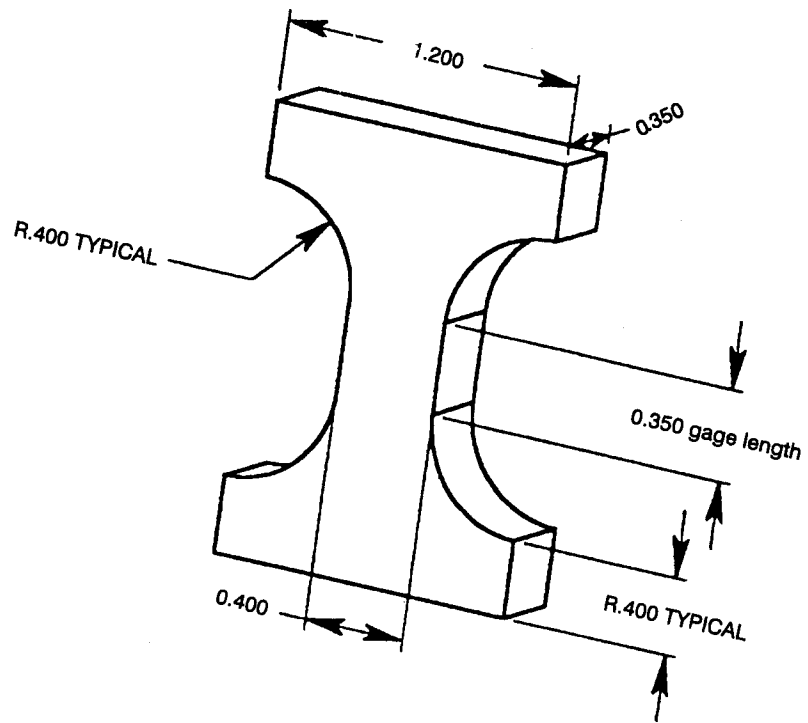


Figure 26. One geometry of a rectangular through-the-thickness specimen.

REFERENCES

1. Stover, D. 1990. "Filament Winding and Fiber Placement: Stretching the Bounds of an Automated Process", *Advanced Composites*, vol. 5, no 6. p. 22 (Nov/Dec).
2. Brunswick Defense, February 1992. Ltr to Mr. J. D. Maltby re: Transducer Shell Information.
3. Maltby, J. D. 1993. "Residual Strain Measurement on Production-Grade Class IV Flextensional Transducer Shell," NRaD Technical Report 1603 (April).
4. American Society for Testing and Materials (ASTM) D 2584-68. 1979. "Test Method for Ignition Loss of Cured Reinforced Resins."
5. American Society for Testing and Materials (ASTM) D 2374-70. 1980. "Test Methods for Void Content of Reinforced Plastics."
6. Adams, D. F., and D. E. Walrath. 1987. "Current Status of the Iosipescu Shear Test Method," *Journal of Composite Materials*, 21(6):494 (June).
7. Ifju, P., and D. Post. 1991. "A Special Strain Gage for Shear Testing of Composite Materials," *1991 SEM Spring Conference on Experimental Mechanics, Milwaukee, WI* (June).
8. Lee, S., and M. Munro. 1990. "Evaluation of Testing Techniques for the Iosipescu Shear Test for Advanced Composite Materials," *Journal of Composite Materials*, 24(4):419 (April).
9. Walrath, D. E., and D. F. Adams. 1983. "Iosipescu Shear Properties of Graphite Fabric/Epoxy Composite Laminates," Report No. UWME-DR-501-103-1, Department of Mechanical Engineering, University of Wyoming, Laramie, Wyoming (NASA Grant No. NAG-1-272) (June).

APPENDIX A

BRUNSWICK DEFENSE SPECIFICATIONS

**BRUNSWICK
DEFENSE**

CERTIFICATION OF CONFORMANCE

Purchase Order Number: LK 0116

Part Number: 5705159P001 Revision: J

Serial Numbers: 184

Tested per Spec No. 5710547, Rev. A, para. 4.3.2 except flexural strength test used .25" nose. Apparent interlaminar shear used 0.5" nose with 0.062" foam pad.

This is to certify that the above referenced assemblies have been fabricated in conformance with applicable contract, specification, and drawing requirements.

 3/27/92

Brunswick Corporation
Quality Assurance Engineer

Table I (cont)

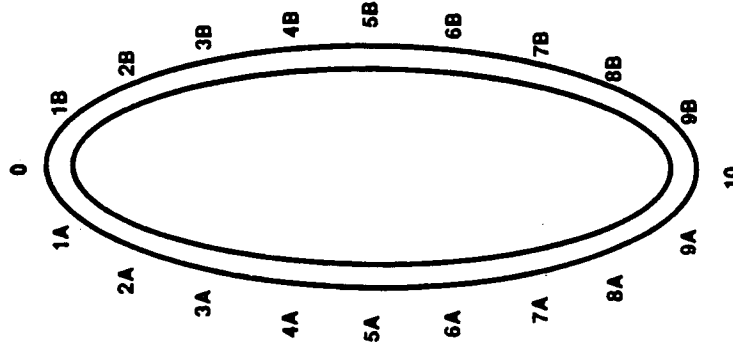
S/N 184

SHELL DASH NO. 2, SIDE A

LOC.	1ST	MIDDLE	3RD
0	2.146	2.140	2.137
1A	2.091	2.084	2.070
2A	2.157	2.151	2.145
3A	2.145	2.139	2.132
4A	2.152	2.138	2.131
5A	2.154	2.154	2.137
6A	2.155	2.147	2.137
7A	2.158	2.148	2.135
8A	2.165	2.165	2.159
9A	2.075	2.074	2.067
10	—	—	—

SHELL DASH NO. 2, SIDE B

LOC.	1ST	MIDDLE	3RD
0	—	—	—
1B	2.068	2.066	2.068
2B	2.162	2.175	2.168
3B	2.149	2.148	2.137
4B	2.162	2.145	2.132
5B	2.154	2.148	2.130
6B	2.157	2.142	2.130
7B	2.158	2.136	2.127
8B	2.161	2.145	2.141
9B	2.088	2.075	2.067
10	2.147	2.130	2.130



PAGE	REV	PART NO.	S/N-L-N-B/N
8	C	230178	107

Pack and Ship

BRUNSWICK DEFENSE Lincoln, Nebraska	QUALITY CONTROL FORM	QCF <u>06-179</u>
	TITLE: Acceptance Testing Report PROGRAM: LTS Composite Shell	Rev. <u>A</u> Page <u>1</u> Eff. Date <u>9-3-91</u> S/N <u>—</u>

LTS
 COMPOSITE SHELL
 PROCESS CONTROL LABORATORY
 BRUNSWICK CORPORATION
 LINCOLN, NEBRASKA

Part Number	<u>174239</u>	Lot Number/Dash Numbers	<u>107-1</u> <u>1</u> <u>107-2</u>
Lab Log Number	<u>25896</u>	Cure Date	_____
Cost Center	<u>19016</u>	Test Date	<u>19 MAR 92</u>

TEST	MINIMUM REQUIREMENTS	TEST RESULTS
Flexural	140 KSI Individual	1. <u>198.8</u>
Strength	160 KSI Average	2. <u>204.1</u>
QCP-06-643		3. <u>207.1</u>
		4. <u>206.5</u>
		Avg. <u>204.125</u>
Interlaminar	11 KSI Individual	1. <u>13.020</u>
Shear	12 KSI Average	2. <u>12.852</u>
QCP-06-643		3. <u>13.078</u>
		4. <u>12.859</u>
		Avg. <u>12.960</u>
Resin	Report Actual	<u>30.13</u>
Content		

[Signature] ☒ Accept ☐ Reject
 Test Technician

Ship S/N's 183 184

Squawk No. _____

APPROVAL	ORIG./ENG	QUALITY/ENG.	PROG. MGR.		
NAME	<u>C. Frank</u>	<u>S. Gross</u>	<u>J. Bursey</u>		
DATE	<u>8/24/91</u>	<u>8/28/91</u>	<u>8-28-91</u>		

BRUNSWICK DEFENSE
LABORATORY
FLEXURAL PROPERTIES OF PLASTICS
ASTM D790 (3 POINT LOADING)

03/19/92
09:46

CUSTOMER	LOCKHEED	TECHNICIAN	G. FRANK
TEST TEMP	75F	SAMPLE I.D.	L/N = 107
LIST DATE	03/19/92	X-HEAD RATE IN/MIN	-.32
REPORT NO.		FILE ID	ES25896
BMS NO.	174239	TPA NO.	
LOWER SPAN (IN)	6	CC/WBS #	19016-62000

COMMENTS: LTS

ID NO	AREA sq in	ULT LBS	X-HEAD (IN)	ULT STRAIN	COMPOSITE STRESS (KSI)	MODULUS (MSI)
1	.1003	367	1.2477	.0403	198.8	5.41
2	.1009	381	1.1677	.0381	204.1	5.4
3	.0996	377	1.2068	.0392	207.1	5.5
4	.1004	381	1.2076	.0392	206.5	5.44
MEAN		376.5	1.207	.039	204.125	5.438
STD		6.606	.033	.001	3.776	.045
CO VAR %		1.755	2.705	2.291	1.85	.828

TESTED BY



BRUNSWICK DEFENSE
LABORATORY
SHORT-BEAM SHEAR METHOD
ASTM D2344

03/19/92
11:46

CUSTOMER	LOCKHEED	TECHNICIAN	G. FRANK
TEST TEMP	75F	SAMPLE ID	L/N = 107
LIST DATE	03/19/92	X-HEAD RATE IN/MIN	-.20
COST CENTER NO.	19016-62000	FILE ID	ES25896
BMS NO.	174239	TPA NO.	
SPAN LENGTH	.76	SPECIMEN LENGTH	1.25

COMMENTS LTS

SAMPLE NO	WIDTH IN	THICK IN	AREA SQ IN	ULTIMATE LBS	HZ SHEAR PSI
1	.268	.19	.05092	884	13020
2	.26	.189	.04914	844	12882
3	.262	.19	.04978	868	13078
4	.256	.189	.04838	830	12859
MEAN					12960
STD					106
CO VAR %					.8

TESTED BY

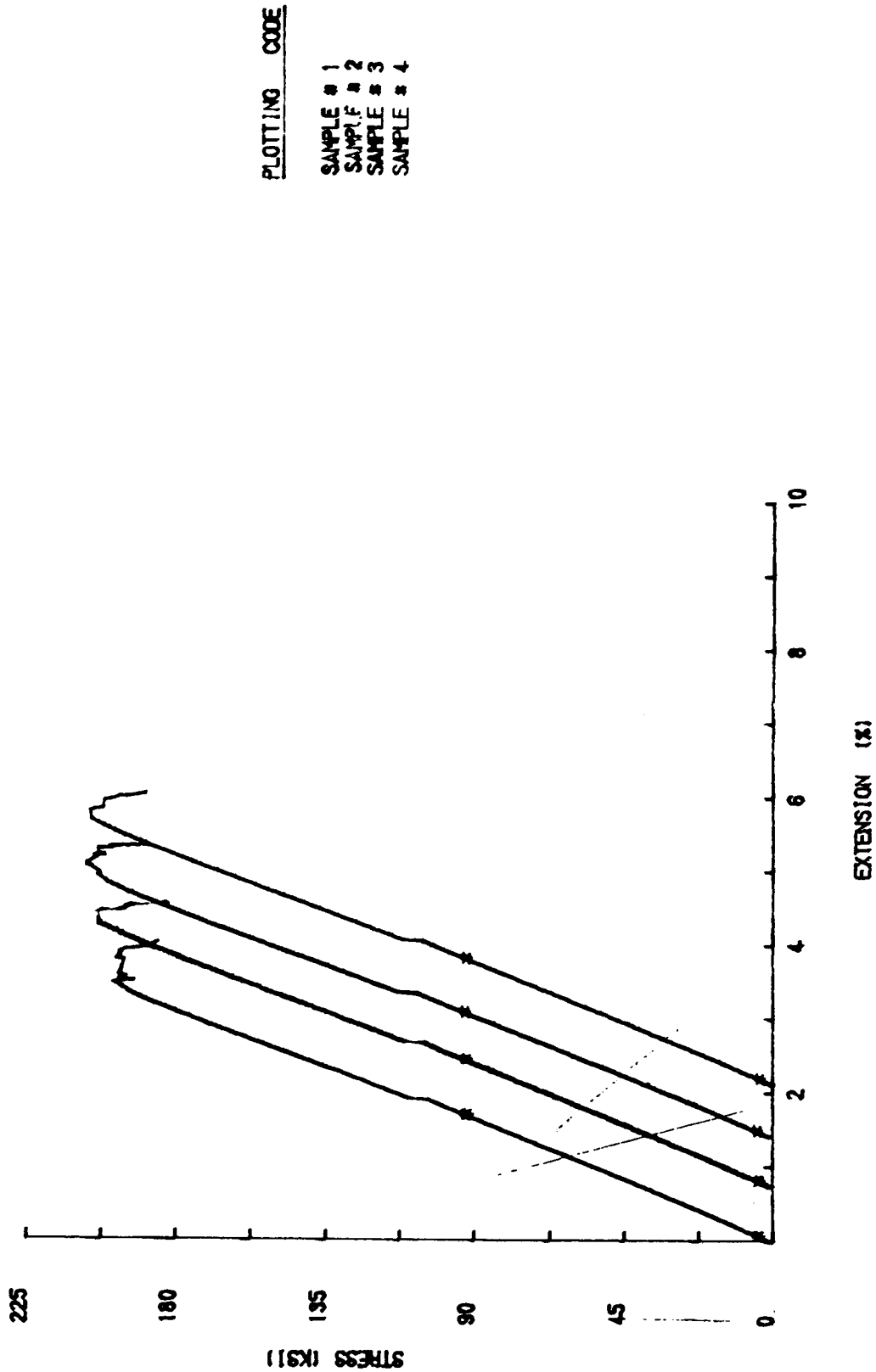


SAMPLE ID : L/N = 107
BNS : 174239
TPA :

COMMENTS : LTS

BRUNSWICK DEFENSE
FLEXURAL PROPERTIES OF PLASTICS
ASTM D790 (3 POINT LOADING)

DATE : 03/19/82
TIME : 09:46
FILE ID : ES25096



DATE : 03/19/92
TIME : 11:48
FILE ID : ES25896

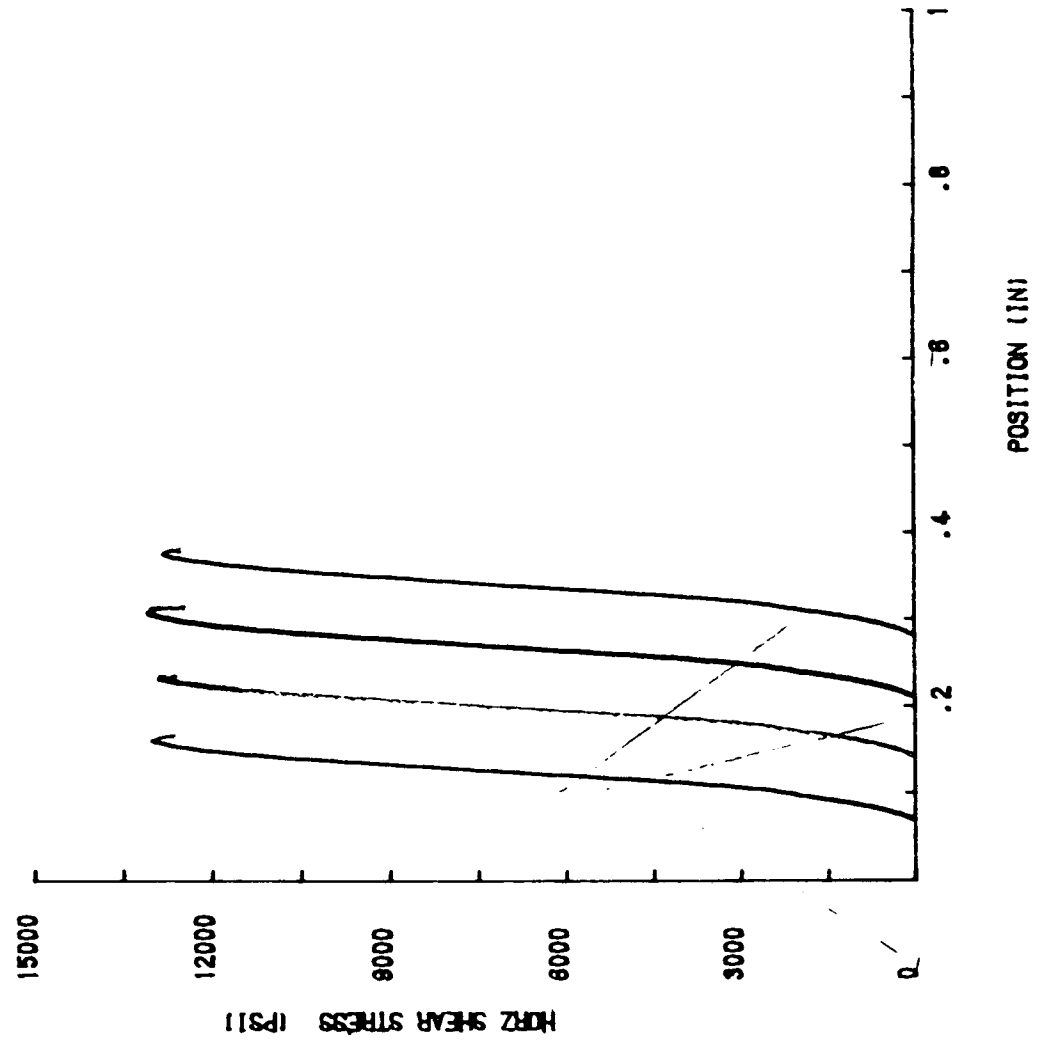
BRUNSWICK DEFENSE
SHORT-BEAM SHEAR METHOD
ASTM D2344

SAMPLE ID : L/N = 107
BMS : 174239
TPA :

COMMENTS : LTS

PLOTTING CODE

SAMPLE # 1
SAMPLE # 2
SAMPLE # 3
SAMPLE # 4



REPORT DOCUMENTATION PAGE			Form Approved OMB No. 0704-0188	
Public reporting burden for this collection of information is estimated to average 1 hour per response, including the time for reviewing instructions, searching existing data sources, gathering and maintaining the data needed, and completing and reviewing the collection of information. Send comments regarding this burden estimate or any other aspect of this collection of information, including suggestions for reducing this burden, to Washington Headquarters Services, Directorate for Information Operations and Reports, 1215 Jefferson Davis Highway, Suite 1204, Arlington, VA 22202-4302, and to the Office of Management and Budget, Paperwork Reduction Project (0704-0188), Washington, DC 20503.				
1. AGENCY USE ONLY (Leave blank)		2. REPORT DATE April 1993		3. REPORT TYPE AND DATES COVERED Final
4. TITLE AND SUBTITLE EVALUATION OF THE PRODUCTION-GRADE CLASS IV FLEXTENSIONAL TRANSDUCER SHELL			5. FUNDING NUMBERS PE: 0602314N WU: DN306254	
6. AUTHOR(S) J. D. Maltby				
7. PERFORMING ORGANIZATION NAME(S) AND ADDRESS(ES) Naval Command, Control and Ocean Surveillance Center (NCCOSC), RDT&E Division San Diego, CA 92152-5001			8. PERFORMING ORGANIZATION REPORT NUMBER TR 1604	
9. SPONSORING/MONITORING AGENCY NAME(S) AND ADDRESS(ES) In-house			10. SPONSORING/MONITORING AGENCY REPORT NUMBER	
11. SUPPLEMENTARY NOTES				
12a. DISTRIBUTION/AVAILABILITY STATEMENT Approved for public release; distribution is unlimited.			12b. DISTRIBUTION CODE	
13. ABSTRACT (Maximum 200 words) This report evaluates the physical characteristics and mechanical properties of the production-grade composite Class IV flextensional transducer shell produced by Brunswick Defense, in Lincoln, NE.				
14. SUBJECT TERMS shear tests shell thickness shear moduli creep characteristics rosette strain gage			15. NUMBER OF PAGES 49	
			16. PRICE CODE	
17. SECURITY CLASSIFICATION OF REPORT UNCLASSIFIED	18. SECURITY CLASSIFICATION OF THIS PAGE UNCLASSIFIED	19. SECURITY CLASSIFICATION OF ABSTRACT UNCLASSIFIED	20. LIMITATION OF ABSTRACT SAME AS REPORT	